



## A Flexible pH-Sensing Structure Using WO<sub>3</sub>/IrO<sub>2</sub> Junction with Al<sub>2</sub>O<sub>3</sub> Encapsulation Layer

Li-Min Kuo,<sup>a,z</sup> Kuan-Neng Chen,<sup>b</sup> Yi-Lin Chuang,<sup>a</sup> and Shuchi Chao<sup>a</sup>

<sup>a</sup>Department of Electrophysics, National Chiao Tung University, Hsinchu 300, Taiwan

<sup>b</sup>Department of Electronics Engineering, National Chiao Tung University, Hsinchu 300, Taiwan

A diode-like current-voltage characteristic in response to hydrogen-ions based on a WO<sub>3</sub>/IrO<sub>2</sub> diode coated with a membrane-like Al<sub>2</sub>O<sub>3</sub> is reported. Microsensors fabricated with the oxides (IrO<sub>2</sub> and WO<sub>3</sub>) will suffer from interference errors in pH-measurements due to their strong responses to environmental redox species. With ionic-conductive and insulation properties, the membrane can mediate the transport of released protons and block the electrons from redox species in solutions. Invoking proton-electron double injection, H<sup>+</sup> and e<sup>-</sup> produce redox reactions, which control the conductivity and preserve the continuity of currents across the interface with a good sensitivity (0.168 μA/pH) between pH = 2 to 12.

© 2012 The Electrochemical Society. [DOI: 10.1149/2.004303ssl] All rights reserved.

Manuscript submitted November 1, 2012; revised manuscript received November 29, 2012. Published December 27, 2012.

Significant attention has been paid to the use of solid-state materials as chemically sensitive devices.<sup>1,2</sup> Gate oxides were used by certain field-effect transistors known for detecting H<sup>+</sup> concentrations instantly.<sup>3</sup> InP/Pt Schottky diode was utilized to make a phenomenological model based on forming electric dipole layer by hydrogen ions in semiconductor applications.<sup>4</sup> A Ni/n-Si Schottky diode using the magnetization of a Ni layer modulates the diffusion rate of H<sup>+</sup> was reported.<sup>5</sup> However, electrical characteristics of solid-state, ion-conducting materials situated in liquids are barely addressed with regard to interfacial or material instability resulting from environmental variability.<sup>6</sup> Practical uses are less attractive due to the lack of a built-in “current turn-on” capacity, as is commonly found in microsensors.<sup>7</sup> Moreover, more sophisticated process flows should be investigated further.

In this letter, a solid-state and chemically sensitive device is proposed to operate as a basis for construction of durable microsensors that are operable in liquids. The sensor exhibits diode-like current-voltage characteristics in response to the presence of H<sup>+</sup>. Microsensors built with the insertion oxides (IrO<sub>2</sub> and WO<sub>3</sub>) will suffer from interference errors in media over pH-span values between 2 and 12. Based on the conception that Al<sub>2</sub>O<sub>3</sub> film is an ionic conductor with electronic insulation property, the encapsulation layer was integrated on the diode surface in this work. Theoretically, the membrane can mediate the transport of released protons and block the transport of electrons from other redox species presented in solutions. According to proton-electron double injection, H<sup>+</sup> and e<sup>-</sup> produce reversible redox reactions, which control the conductivity and preserve the continuity of current across the interface without incidences.

### Experimental

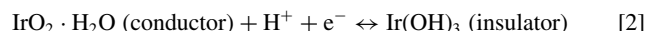
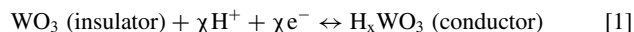
As depicted in the inset (a) of Fig. 1, a pair of Pt-electrodes and sputtered WO<sub>3</sub> and IrO<sub>2</sub> films were fabricated by using procedures described earlier.<sup>8</sup> Initially, a n-type 4-inch silicon substrate was cleaned with piranha solution (H<sub>2</sub>SO<sub>4</sub> :H<sub>2</sub>O<sub>2</sub> = 3:1) at 80°C for 20 min, followed by a DI-water rinse for 5 min and a dry N<sub>2</sub>-flow purge. A SiO<sub>2</sub> layer (2000 Å) was deposited on the Si-substrate, followed by a LPCVD deposition (Si<sub>3</sub>N<sub>4</sub> 4000 Å). Next, 50 Å of chromium, followed by 1200 Å of Pt, was deposited on the Si<sub>3</sub>N<sub>4</sub> film by a dual electron-beam evaporator and then patterned using a lift-off technique. The Pt-electrodes, separated by distance of 400 μm, were 600 μm wide and 1400 μm long. An RF-sputtering of the WO<sub>3</sub> target (99.99%, 4.77 g/cm<sup>3</sup>) was carried out (35% O<sub>2</sub> in Ar) at a pressure of 45 mTorr and temperature of 100°C. After acetone clean, DI-water rinse and a dry N<sub>2</sub> gas purge, annealing process was achieved in a high-temperature (350°C) chamber at a pressure of 15 mTorr for 3.5 hr. The IrO<sub>2</sub> film was fabricated using an Iridium target (99.95%, 21.8 g/cm<sup>3</sup>)

and carried out at a pressure of 60 mTorr (50% O<sub>2</sub> in Ar) by a sputtering approach. Next, the Al<sub>2</sub>O<sub>3</sub> film was fabricated using sputtering of an Al<sub>2</sub>O<sub>3</sub> target (99.99%, 3.26 g/cm<sup>3</sup>) and carried out at a pressure of 70 mTorr (50% O<sub>2</sub> in Ar) for 1.5 hr using a magnetron sputtering. All sputtering films were patterned by a lift-off technique. The thickness of WO<sub>3</sub>, IrO<sub>2</sub>, and Al<sub>2</sub>O<sub>3</sub> films were 3000 Å, 1200 Å, and 250 Å, respectively, as measured using an alpha-step stylus instrument. Electrical contacts to individual Pt-electrodes were made using Ag-epoxy (FA-705, Fujikura Kasei). An encapsulation process followed, using insulating epoxy (K-22 Conap) to prevent short circuits, which was cured to become solid in an oven at 150°C for 30 min. The reaction region was surrounded and encapsulated by the insulating epoxy resin.

Before measurements commenced, a two-point calibration was processed using three known pH-calibration buffers (pH = 4, 7 and 10) and then pH-meter (SA-250, Orion) indications were corrected accordingly. The sample solutions were prepared using Britton-Robinson buffer solution, which consisted of 0.04M H<sub>3</sub>BO<sub>3</sub>, 0.04M H<sub>2</sub>PO<sub>4</sub> and 0.04M CH<sub>3</sub>COOH; eleven samples were titrated to the desired pH-value (from pH = 2 to 12) with 0.2 M KOH pseudo-randomly dropping. The device packaged into an integral flow cell was tilted 30° to allow exposure to solutions and was implemented to be a smooth flow path of the solution supplied. The sample solutions were supplied by the flow rates from a microprocessor-controlled peristaltic pump (Rainin RP-1) with 3 rpm and Tygon tube (3.18 mm diameter) connected with a glass tube. The pH-sensor was connected to a Keithley 617 source-measure unit via Keithley Cable 6011 wires as simplified in the inset (b) and (c) of Fig. 1. All potentials measured were relative to Hg/Hg<sub>2</sub>Cl<sub>2</sub> (z11311-5, Aldrich) electrode. A GPIB (General Purpose Interface Bus) and a LabView-based program were employed for recording the experimental results.

### Results and Discussion

This study was inspired by the earlier work, as on a bicarbonate (HCO<sub>3</sub><sup>-</sup>)-doped, PVA (polyvinyl alcohol), solid-polymer matrix interfaced with the contact of WO<sub>3</sub> and IrO<sub>2</sub>, which can respond to CO<sub>2</sub> gas via detection of H<sup>+</sup>.<sup>8</sup> Based on pH-sensitive properties of WO<sub>3</sub> and IrO<sub>2</sub>, the device will interact with H<sup>+</sup> in redox reactions.<sup>9</sup> Both WO<sub>3</sub> and IrO<sub>2</sub>-reductions to conducting H<sub>χ</sub>WO<sub>3</sub> (0 < χ < 0.5) and insulating Ir(OH)<sub>3</sub>, respectively (reactions 1 and 2). These redox transformations result from the insertion of ionic species into the oxides, which can produce large conductance changes.<sup>10,11</sup> IrO<sub>2</sub> · H<sub>2</sub>O and Ir(OH)<sub>3</sub> are solid-state materials, and their concentrations will be easily affected as they are oxidized or redox by other materials.



In Fig. 1, the current-voltage characteristics of the sensor were measured by a Keithley 236 source-measure unit. The diode undergoes

<sup>z</sup>E-mail: lmkuo.ep97g@nctu.edu.tw

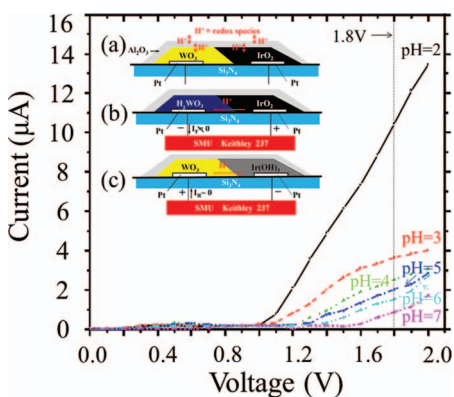


**Figure 1.** The I-V Characteristics of our pH sensor under the forward bias with different pH-levels (pH = 2 to 7). (The inset (a), (b) and (c) show no-biased, forward-biased and reverse-biased diode based on the contact WO<sub>3</sub> and IrO<sub>2</sub> on Si under H<sup>+</sup> modulation).

a current increase in the forward direction as the pH-level is decreased. This behavior is consistent with the WO<sub>3</sub> and IrO<sub>2</sub> redox processes (reactions 1 and 2) and electrochemical potentials in both reactions become more positive in more acidic environments. The inset (b) and (c) in Fig. 1 illustrates the forward and reverse-biased diodes under H<sup>+</sup> modulation schematically. Invoking proton-electron double injection, WO<sub>3</sub> film was reduced to H<sub>x</sub>WO<sub>3</sub> by the combination of electrons from the Pt-electrode and H<sup>+</sup> through the Al<sub>2</sub>O<sub>3</sub> layer. Under a fixed bias of 1.8 V applied to the sensor, the current response versus pH-level change with an interval step of pH = 1 and from pH = 2 to 12,

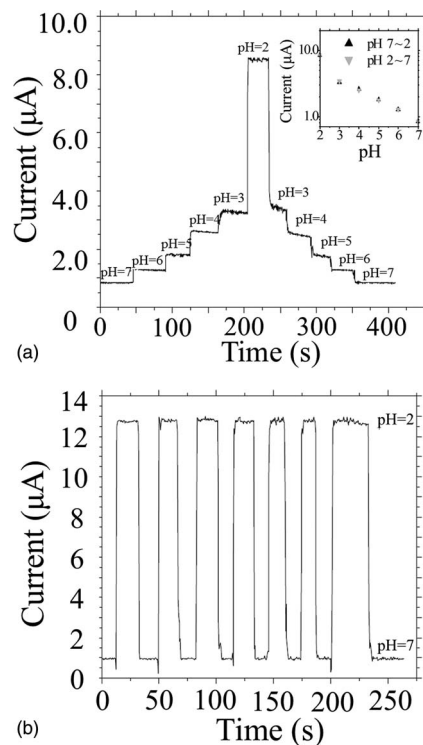


**Figure 3.** (a) Stepwise current response of our pH sensor to different pH-level from pH = 2 to 7 and pH = 7 to 2. (b) Stepwise Current response of our pH sensor from pH = 2 to 7 and pH = 7 to 2 after switching with seven times.

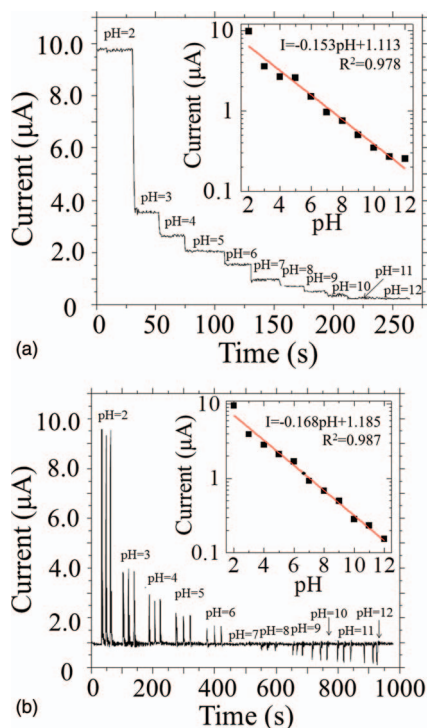


**Figure 2.** (a) Current response versus pH-level change with an interval step of pH = 1 and from pH = 2 to 12. (Inset shows a linear fitting slope of logarithmic current versus different pH-level) (b) Pulse current response of the pH sensor versus pH-level change with the interval step of pH = 1 from pH = 2 to 12. (Inset shows a linear fitting slope of logarithmic current and different pH-level according to the average of three peak-current values) The response and recovery time are defined as 20% to 80% of the rising and falling edge in the transient response.

as shown in Fig. 2a. The repeatability experiments were measured by three sequential droplets (1 mL per droplet) for each pH value. The next dropping followed up after the current value of the previous dropping was attenuated and settled down, as shown in Fig. 2b. Three peak-current values in each pH-level are almost identical. The maximum ramp-up time is 1.5 sec and the recovery time is within 7 sec. The rising and falling time in the transient response are longer than others due to more H<sup>+</sup> in the solution will produce a thicker Helmholtz layer generated at the interface of the encapsulation layer and the diode.<sup>12</sup> The larger parasitic capacitance and resistance will be produced at the interface and the response time will be increased.

In Fig. 3a, the reproducibility of the pH-sensor was shown by the measurement of a stepwise increase and decrease between pH = 2 and 7. The duration for each condition were applied about 40 sec. From Fig. 3a, it is apparent that the sensor provides excellent reversibility in the dynamic response transients. The discrepancy between the forward (pH = 7 to 2) and backward (pH = 2 to 7) sequential measurements is as slight as negligible as shown in the inset of Fig. 3a. Several switches between pH = 2 and pH = 7 performs the reliable repeatability according to the identical current values as shown in Fig. 3b. The hysteresis is commonly existed in metal-oxide films for the pH-sensing, and substantially depends on the operation in each experiment, the material quality and fabrication batches.<sup>13</sup> The potential drift of the hysteresis may be due to dynamic processes of ion neutralization called the effect of liquid junction potential.<sup>14</sup>

N<sub>2</sub> and O<sub>2</sub> gas were supplied in buffer solutions to prepare N<sub>2</sub> and O<sub>2</sub>-abundant solutions, which may produce voltage fluctuations caused by some factors such as the oxidation states from incomplete oxidation and surface ion exchanges in IrO<sub>2-x</sub> film.<sup>13</sup> These non-ideal effects will generate surface charge-variations with time and the new equilibrium after each reaction.<sup>15</sup> In Fig. 4, the current response shows slight and negligible deviations according to the comparison of N<sub>2</sub> and O<sub>2</sub>-abundant solutions of pH = 2, 6 and 12 at room temperature. The notches in Fig. 4 were due to the air bubble used for the separation during the solution rotations in the experiment.

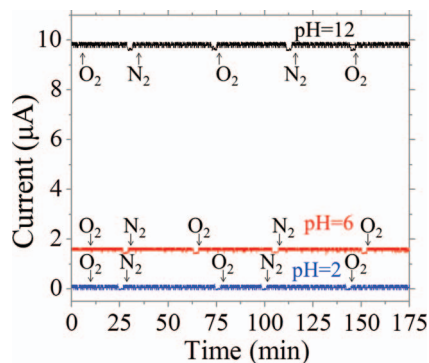


**Figure 4.** Current response of our pH-sensor measured in  $N_2$  and  $O_2$  saturated solution. (pH = 2, 6, and 12)

### Conclusions

In conclusion, a new pH-sensor made of a sputtering  $WO_3/IrO_2$  diode sealed thoroughly by an  $Al_2O_3$  encapsulation layer in response to the presence of hydrogen-ions ( $H^+$ ) has been investigated. With the inherently robust immunity to  $O_2$  perturbation, the encapsulation layer of  $Al_2O_3$  film fully covered the  $WO_3/IrO_2$  diode and prevented  $IrO_2/Ir[OH]_3$  from being increased as oxidized by  $O_2$ . By proton-electron double injection,  $H^+$  and  $e^-$  produce redox reactions, which

control conductivity. The solid-state sensor exhibits good stability, repeatability, and reversibility in various pH environments ranging from 2 to 12 at room temperature. This chemically sensitive device will be useful as a basis for construction of durable microsensors for tracing the acidity in environmental and biological applications.

### References

1. M. Wanunu and A. Meller, *Nano Lett.*, **7**, 1580 (2007).
2. T. Ueda, V. V. Plashnitsa, M. Nakatou, and N. Miura, *Electrochem. Commun.*, **9**, 197 (2007).
3. M. W. Shinwari, M. J. Deen, and D. Landheer, *Microelectronics Reliability*, **47**, 2025 (2007).
4. T. Kimura, H. Hasegawa, T. Sato, and T. Hashizume, *Jpn J. Appl. Phys.*, **45**, 3414 (2006).
5. A. Salehi and V. Nazerian, *Sens. Actuators B*, **122**, 572 (2007).
6. J. W. Gardner, *Microsensors, Principles and Applications*, p. 235, John Wiley & Sons, Chichester (1994).
7. N. Leventis, M. O. Schloh, M. J. Natan, J. J. Hickman, and M. S. Wrighton, *Chem. Mater.*, **2**, 568 (1990).
8. J. C. Lue and S. Chao, *Jpn J. Appl. Phys.*, **36**, 2292 (1997).
9. B. Scrosati, *Applications of electroactive polymers*, p. 251, Chapman & Hall, London (1993).
10. K. Pa'sztor, A. Sekiguchi, N. Shimo, N. Kitamura, and H. Masuhara, *Sens. Actuators B*, **12**, 225 (1993).
11. M. J. Natan, T. E. Mallouk, and M. S. Wrighton, *J. Phys. Chem.*, **91**, 648 (1987).
12. J. Lyklema, *Fundamentals of Interface and Colloid Science*, **2**, 3.208 (1995).
13. A. Fog and R. P. Buck, *Sens. Actuators*, **5**, 137 (1984).
14. W. D. Huang, H. Cao, S. Deb, M. Chiao, and J. C. Chiao, *Sens. Actuators A*, **169**, 1 (2011).
15. W. Olthuis, M. A. M. Robben, P. Bergveld, M. Bos, and W. E. Linden, *Sens. Actuators B*, **2**, 247 (1990).